Non Destructive Testing of sandwich composites: adhesion defects evaluation; Experimental and Finite Element Method simulation comparison

Elhadji Barra Ndiaye, Hugues Duflo

ACOUSTICS 2012

Non Destructive Testing of sandwich composites: adhesion defects evaluation; Experimental and Finite Element Method simulation comparison

E.B. Ndiaye and H. Duflo

Laboratoire Ondes et Milieux Complexes,
elzobarz@hotmail.com

Control and detection of defects like disbond and delamination in sandwich composite material is important today in aerospace industry. For experimental investigation, disbonding was introduced at different locations in sandwich composite by insertion of a Teflon film between honeycomb and the glue film, or by suppression of glue on small area (before curing process). The A_0 Lamb mode was excited close to 550 kHz frequency. The transmitted and reflected wave signals were detected by velocimetry laser after interacting with the structure, and the boundaries of the honeycomb. A Finite Element Method simulation is also computed to simulate behavior of the Lamb wave in case of disbond area. Good correlation between the experimental and FEM simulation results was observed. The results demonstrate the effectiveness of Lamb waves to detect delamination or disbonding in sandwich composite material.

1 Introduction

This paper deals with Non Destructive Testing NDT of sandwich honeycomb structures which are widely used in aerospace industry. They are made of two face sheets in composite (skins) and between is inserted an aluminium honeycomb by bonding. However an intensive load or cycle loading can induce debonding at the interface between the core and skin plates, threatening the structural health of the material. Reinforcing fibers give composites the attributes of high strength and stiffness which translates to high performance. Due to the complex nature of this kind of structure, an understanding of the guided wave propagation mechanism at low frequency imposes many challenges.

A numerical simulation is first conducted to investigate the wave propagation mechanism in honeycomb beam by using the imposed displacements in the boundaries of the structure as a transducer excitation. In order to understand guided Lamb waves propagation for detecting defects such as debonding or delaminations, we have to solve the problem numerically by considering a 2D modelisation of the structure. Some works was being done about this study [1, 4].

To compare the numerical results, a spectral analysis will be done in the second part of this works by using a laser vibrometer detection [5, 6]. This experimental study is carried out at 550 kHz in real sandwich honeycomb by evaluating attenuation of the wave propagation along these materials.

2 Guided waves propagation: theory

2.1 Definition

The Lamb waves propagate on long distances in structures according to materials and their thicknesses. They propagate by producing small deformations within the material. As other waves, Lamb modes are characterized by amplitude, frequency and a speed of propagation. There are two families of Lamb waves: the symmetric modes S and the asymmetric modes A. Lamb modes are numbered by 0, 1, 2,... n according to their order of appearance and their nature, symmetric or asymmetric when we increase in term of frequency. The analytical description of Lamb waves in anisotropic medium is indispensable to understand the results of numerical simulations or experimental propagation of ultrasonic waves in sandwich materials. The calculation allows obtaining dispersion curves is described follow.

2.2 Waves in anisotropic solid

Before developing a numerical code and an experimental investigation of waves in anisotropic plates, we make an overview of studies about this phenomenon. The governing equations of wave propagation in a single laminated composite (plate) and sandwich composites are introduced and their dispersion curves permit to identify what waves are suitable at a given frequency to investigate a material.

Nayfeh and Rose have widely studied waves propagation in laminated composites [7,8]. The plate is assumed infinite in the x_1 and x_2 direction, x_3 is normal to the plate (Figure 1).

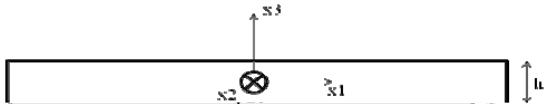

Figure 1: Plate sample description

Waves propagate according to the x_1 direction. We can obtain this case by making a rotation around the x_3 axis of the matrix of rigidity of the material. The plate being infinite in the x_2 direction and the waves propagating according to x_1, the displacements are independent from the coordinate x_2 (we find the hypothesis of the plane strain). The equation of motion is obtained from the governing equation of wave propagation in an arbitrary medium

$$\rho \frac{\partial^2 u_i}{\partial t^2} = \frac{\partial \sigma_{ij}}{\partial x_j}, \tag{1}$$

and in the three principal axes, it can be expanded as

$$\begin{aligned} \rho \frac{\partial^2 u_1}{\partial t^2} &= \frac{\partial \sigma_{11}}{\partial x_1} + \frac{\partial \sigma_{12}}{\partial x_2} + \frac{\partial \sigma_{13}}{\partial x_3} \\ \rho \frac{\partial^2 u_2}{\partial t^2} &= \frac{\partial \sigma_{21}}{\partial x_1} + \frac{\partial \sigma_{22}}{\partial x_2} + \frac{\partial \sigma_{23}}{\partial x_3} \\ \rho \frac{\partial^2 u_3}{\partial t^2} &= \frac{\partial \sigma_{31}}{\partial x_1} + \frac{\partial \sigma_{32}}{\partial x_2} + \frac{\partial \sigma_{33}}{\partial x_3} \end{aligned}. \tag{2}$$

The displacement field u_i in the x_1, x_3 direction is expressed as

$$u_i = U_i \, \mathrm{e}^{ik(x_1 + \alpha x_3 - ct)}, \tag{3}$$

where U_i is the amplitude corresponding to the different displacement components, k the wavenumber corresponding to the x_1 direction, α is the ratio of the wavenumber along the x_3 direction over that of the x_1 direction, c is the phase velocity. We can see that Eq.(3) is independent of the x_2 direction. So finally we obtain the dispersion equation

$$\begin{aligned} S &= D_{11}G_1 \cot(\gamma\alpha_1) - D_{13}G_3 \cot(\gamma\alpha_3) + D_{15}G_5 \cot(\gamma\alpha_5) \\ A &= D_{11}G_1 \tan(\gamma\alpha_1) - D_{13}G_3 \tan(\gamma\alpha_3) + D_{15}G_5 \tan(\gamma\alpha_5) \end{aligned}. \tag{4}$$

D_{ij}, G_i and γ are mechanical characteristics of the material, a numerical resolution of Eq. (4) in FORTRAN ® allows to plot the dispersion curves of Lamb waves of a carbon fiber reinforced composite CFRP plate whose elastic constants (unit: GPa) are mentioned in table 1.

Table 1: Elastic constants, density and CFRP thickness

C11	C13	C33	C55	ρ(Kg/m3)	h(mm)
56.7	9.87	14.7	4.11	1530	1.6

Information about the initial estimated points are given by the maximum frequency of the window. Indeed, with this frequency, all modes existing in the window are visible. With certain values of velocity distributed linearly between both extreme velocities of the domain of study, we look for a zero of the determiner of the system (with Newton Raphson's method). The obtained different zeros correspond each to the first point of a mode.

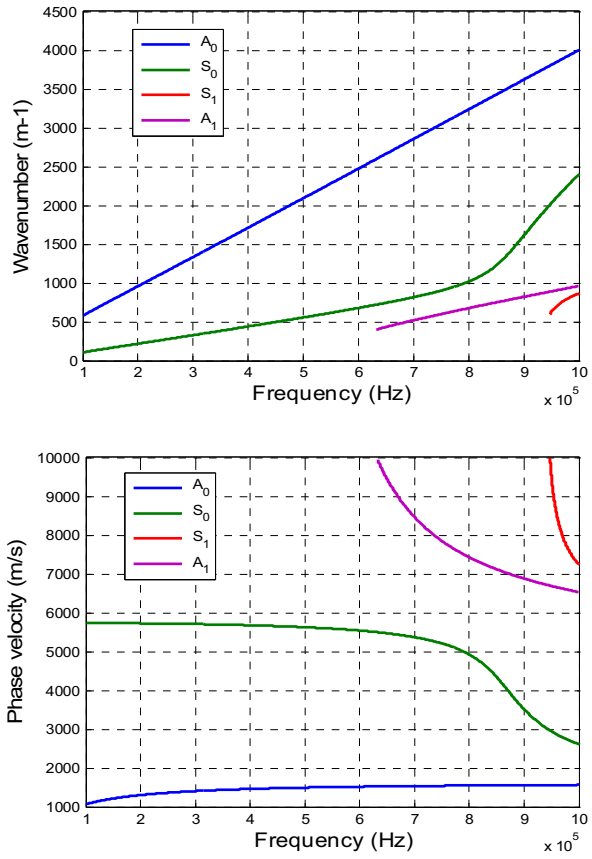

Figure 2: Dispersion curves of a CFRP composite with 1.6mm thick; up (wavenumber), down (phase velocity)

We can see that an assumption is made between the plate and the honeycomb sandwich panel on the propagation of Lamb waves. This hypothesis has been done in some studies [2], the acoustic impedance of the skin material is "harder" than the acoustic impedance of the honeycomb. Indeed, the high core to skin thickness ratio allows considering a Lamb wave propagation in the skin.

3 Finite Element Simulation

The software with which we work to simulate the behavior of waves in the structures to be assessed is COMSOL MULTIPHYSICS® in particular its 3.5a version, which is a commercially available finite element based program for simulating single and multiphysics applications. The structural mechanics module and temporal analysis are chosen for this study. Its principle bases on the technique of calculation based on the method of the finite elements which allows defining complex geometries of structures and/or defects.

3.1 Modeling and material properties

Sandwich structure as described above, is made by inserting a light aluminum honeycomb between two composite plates. Figure 3 shows the FE model of a honeycomb sandwich structure with four damping areas called PML (Perfectly Matched Layer) joined with the upper and lower skins [3]. They are very useful during the simulation process; they didn't reflect waves reflected by the aluminum cells.

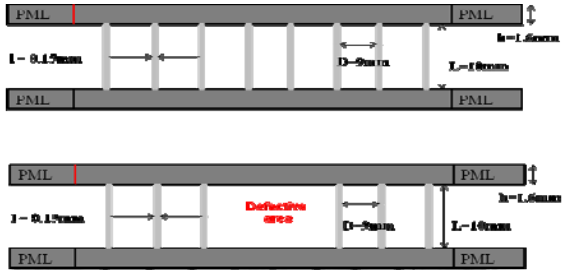

Figure 3: 2D honeycombs sandwich model with PMLs; up (non-defective), down (defective)

For the 2D Lamb wave simulation of this study, the material properties are also given in table 1. Two elements are indispensable or crucial for the simulation of Lamb waves, the meshing and the temporal sampling.

It's necessary to have ten elements (mesh size) per wavelength. Meshes are finer in the modelized structure than in the PMLs, two methods of meshing are used. The first one is a quadrilateral mapped meshes and the second one a triangular meshing. In the first case, subdomains are bounded by four segments (a rectangle); this kind of meshing is adapted for symmetric problems such as a single plate. For complex domains or irregular geometries, triangular meshes are suitable to be used.

The temporal sampling must be defined before starting the simulation; it consists of calculating a step $\Delta t = \frac{\Delta x}{V}$ where V is the phase velocity of the simulated wave. To confirm the best temporal step for our study, the chosen criterion of optimization is the good concordance between the dispersion curves of Lamb waves obtained by FE simulation and those seen in the previous part. Results are very satisfactory by setting $\Delta t = \frac{T}{48}$ where $T = \frac{1}{F}$ is the temporal period at the given frequency (F=550 kHz).

3.2 Simulations and results

Lamb modes are generated in FEM simulation by theoretical displacements. The relative displacements of every mode are calculated in any point in a right section of the structure. At the first extremity of the upper skin (red boundary Figure 3), we impose the normal component U_X and the tangential U_Y of the displacements. They are respectively identified with 2 polynomials of degree 7

PU_X (x_3) and PU_Y (x_3), which are multiplied with an oscillation function of time to obtain R_X and R_Y as:

$$R_x = PU_x(x_3)*(t<30e-6)*\cos(2\pi.550.10^3 t).(t \geq 0).(t \leq 20.10^{-6}).([1-\cos(2\pi/20.10^{-6} t)]/2) \quad (5)$$
$$R_y = PU_y(x_3)*(t<30e-6)*\sin(2\pi.550.10^3 t).(t \geq 0).(t \leq 20.10^{-6}).([1-\cos(2\pi/20.10^{-6} t)]/2)$$

R_X and R_Y derivate from the Dirichlet boundary condition. The $Hu = R$ mode must be used to obtain this kind of excitation. It means that at the end of the excitation (t>30µs), the edge (red boundary) does not reflect any waves which are absorbed by the left PLM. Figure 4 shows this two functions R_X and R_Y, we can see that they vary in quadrature of phase and to obtain a quasi-harmonic regime, 10 periods are applied. The geometrical values of the structure are 200mm length, 1.6mm thick of each plate (skin), 9mm honeycomb distance D, with a 0.15mm width for aluminum. The duration of the excitation's signal is 20µs and all the simulation 150 µs. This signal is then multiplied by zero if t is not in the temporal window (0 à 20 µs) and finally it's again multiplied by a Hamming window.

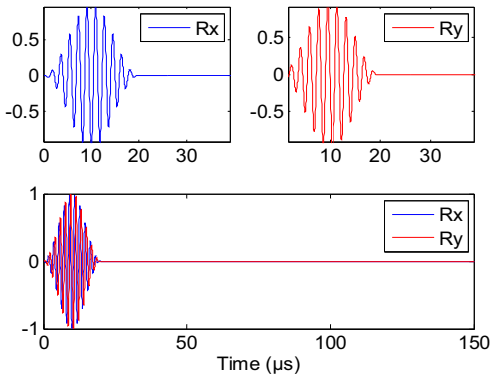

Figure 4: Ten-cycle tone bursts for the excitation

The post-treatment done after the simulation consists of extracting the normal displacements U_Y on a line corresponding to the superior surface of the upper skin. The purpose of this treatment is to get closer to futures experiences with a laser velocimeter which allows exactly detecting vibrations at the surface of an exited plate.

To verify that we have generated a Lamb mode which propagates along the structure, we can plot the temporal evolution of the excited signal at x=0.025m (Figure 5). The incident signal (Hamming) with the reflected waves are observed at this position.

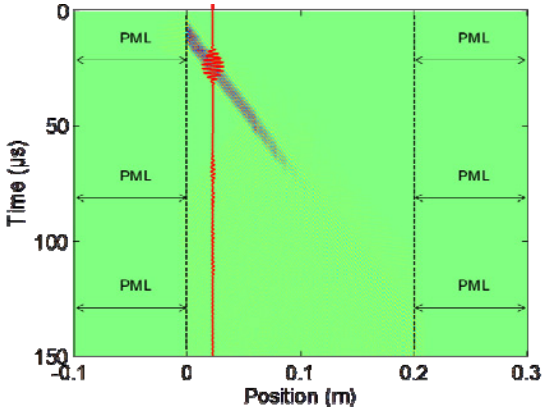

Figure 5: Normal displacements on the upper surface and temporal evolution at x= 0.025m (red line)

In order to compare numerical results with those experimental presented after, we make a spectral analysis.

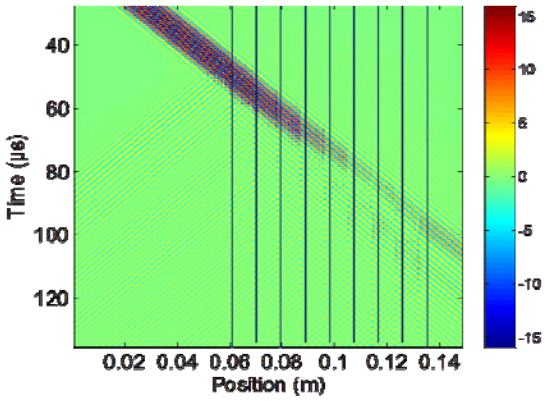

Figure 6: Normal displacements on the upper surface of the non-defective honeycomb sandwich

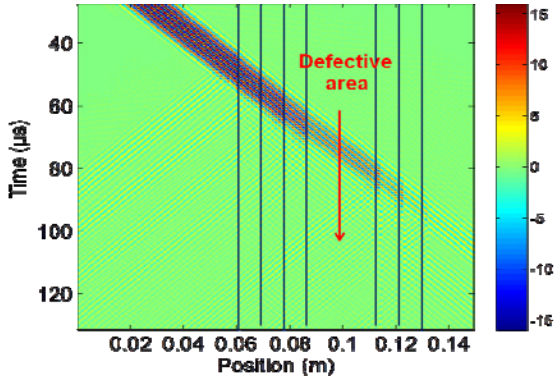

Figure 7: Normal displacements on the upper surface of the defective honeycomb sandwich

The aim of this signal processing is to evaluate the attenuation's coefficient and make some comparisons.

First a temporal fft of the space-time collection $s_1(x,t)$ is done, we obtain $s_1(x,f)$ a frequency spectrum which confirm that the A_0 wave is propagating at 550kHz with a value of wavenumber equals to $2345m^{-1}$.

Second, another fft (Short-Time Fourier Transform) is applied to $s_1(x,f)$ and then we obtain $s_1(x,k)$ where k is the wavenumber of the propagating wave. This transformation is also called Short Space Sliding Fourier Transform.

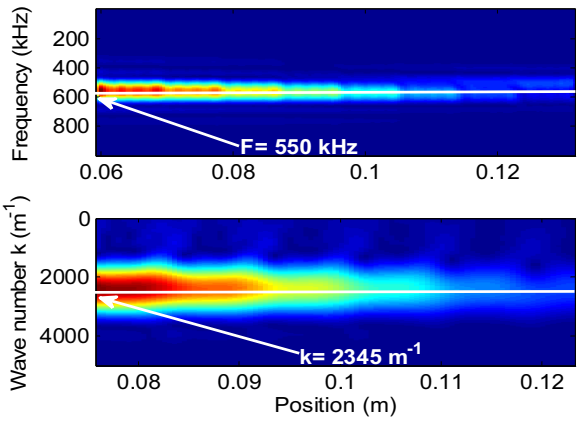

Figure 8: Frequency-position and wavenumber-position images (non-defective honeycomb sandwich)

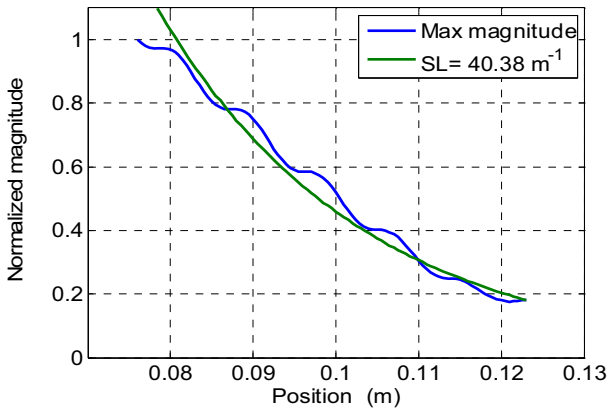

Figure 9: Evaluation of the wave's attenuation coefficient

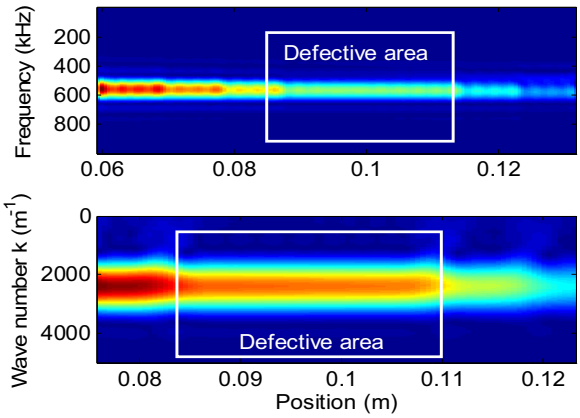

Figure 10: Frequency-position and wavenumber-position images (defective honeycomb sandwich)

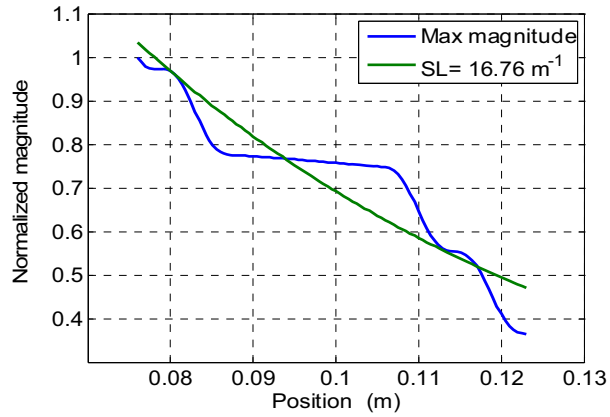

Figure 11: Evaluation of the wave's attenuation coefficient

To evaluate the attenuation of the propagating wave, only the incident signal is considered. This means, firstly to do a 2D fft of the incident signal and secondly a 2D ifft (inverse fft) then we can separate the incident wave and the reflected one.

The magnitude of this 2D fft at the wave number position is plotted in blue and for obtaining the attenuation's coefficient of this propagated wave, a fit of this curve is done. The attenuation is corresponding to an exponential function (exp(-kx)). The slope of this fit (green curve) represents this value and in this case, it equals to k=40.38 m^{-1} for the non-defective simulated sandwich (Figure 9).

The same treatment is done for the defective simulated honeycomb sandwich beam, the value of this attenuation's coefficient equals to 16.76 m^{-1} (Figure 11).

4 Experimental study

4.1 Samples and experimental setup

In this part, two samples of real honeycomb sandwich beam are investigated by the propagation of Lamb wave in air. They are made in CFRP composite with a light aluminum honeycomb as simulated before (Figure 2).

The typical honeycomb sandwich beams to be tested are samples which may be used in some aeronautical parts. The first one, named "G01" is "healthy", without defect. In the middle of the other one, named "G02", a Teflon film is inserted to simulate disbonding. The geometrical characteristics of these samples are: total length 300mm, width 170mm, the total height of the structure is 13.2mm by taking into account 1.6mm thick of each skin and 10mm of the honeycomb.

Experimental studies have been done by the propagation of Lamb waves on air by using a laser velocimeter to detect the vibrations in the surfaces of the structures. The experimental dispositive for the activation and acquisition of Lamb wave signals is described in figure 12.

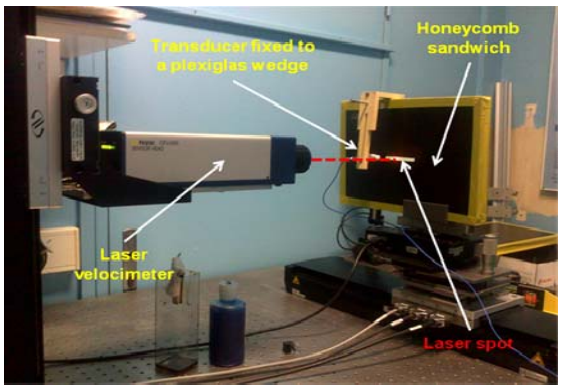

Figure 12: Experimental setup

A generator delivers Ten-cycle sinusoidal tone bursts enclosed in a Hanning window to a Krautkramer transducer. This signal is before amplified, the Lamb waves, produced by the wedge method (60° plexiglas wedge), propagate along the surface and the signal is captured by the laser velocimeter by interferometry. These measurements are performed along a line parallel to the incident Lamb wave propagation direction. This vibrometer integrates a YAG laser which delivers a high power beam (100mW), allowing measurements of materials such composite plate with poor surface quality. The laser translation is controlled by a computer and surface displacements measured at each position are registered in 6250 points signal. In order to improve the signal to noise ratio we perform an averaging on 128 successive shots.

4.2 Results

The same signal processing (i.e. spectral analysis in the space domain) is made to assess debonding in the case of this two honeycomb sandwich samples. For each sample, the head of the vibrometer laser is translated from x=-30 to

30mm by 0.1mm step (x=0 is the center of the defect for the defective sample, Figure 14).

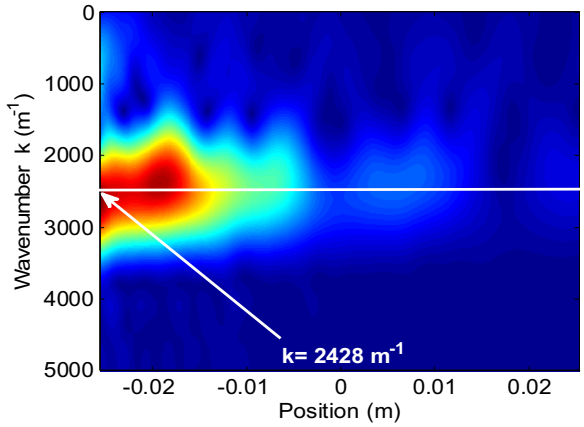

Figure 13: Experimental measurement; wavenumber-position of the G01 sample

As mentioned above in the G02 sample a film of Teflon with 24mm of diameter is inserted in the middle. The defective area is clearly detected and the S_0 wave is slowed down. This is due to thickness of Teflon film.

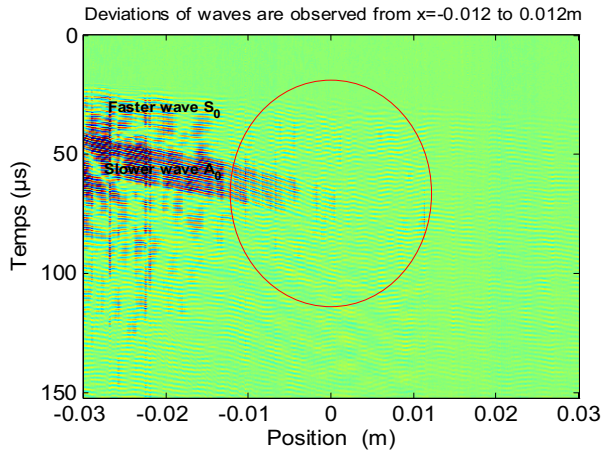

Figure 14: Results for guided Lamb waves interaction with the defective sample G02

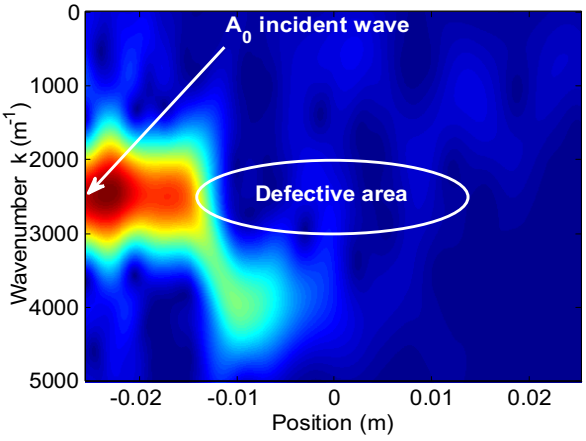

Figure 15: Experimental measurement; wavenumber-position of the G02 sample

We obtain a value of wavenumber equals to 2428 m^{-1} for the sample G01 and 2440 m^{-1} for G02. The evolution of the wave number in the G01 presents no discontinuity so no break of impedance it is only attenuated during the propagation.

For the G02 sample, the intensity of the wavenumber at k=2440m^{-1} disappears completely from x=-0.012 to 0.012m (change of impedance of the medium due to the presence of the Teflon film). We know previously that the defect was introduced between the skin and the honeycomb in the middle of the structure. We conclude that Lamb waves have travelled the disbond area. The Teflon film hasn't the same influence as a disbonding area, because it has a small thickness, and the Lamb wave is sensibly modified. More this confirm the defect size value of 24mm diameter given by the manufacturer.

5 Conclusion

The effectiveness of Lamb waves to detect adhesion's disbond is demonstrated by a FEM simulation and experimentally in this study. The propagation of the first asymmetric mode A_0 through the walls of the honeycomb has allowed us to get an idea on the crossed media.

However, a treatment by fft with a sliding window of the incident wave (by removing first the multiple reflections at the junction of the honeycomb) allows to view the medium in the (k,x) space and in the case of a real defective sample, the size of the defect.

Signal analysis is also applied to experimental results. The waves are easily separated. The defect is also detected.

References

[1] S. Mustapha, L. Ye, D. Wang, Y. Lu, "Assessment of debonding in sandwich CF/EP composite beams using A_0 Lamb waves", Composite Structures 93, 483-491 (2011)

[2] N. Bourasseau, E. Moulin, C. Delabarre, P. Bonniau, "Radome health monitoring with Lamb waves: experimental approach", NDT&E International 33, 393-400 (2000)

[3] S. Delrue, K. Van Den Abeele, "Three-dimensional finite element simulation of closed delaminations in composite materials", Ultrasonics 52, 315-324 (2012)

[4] M. Yang, P. Qiao, "Modeling and experimental detection of damage in various materials using the pulse-echomethod and piezoelectric sensors/actuators", Smart Mater. Struct. 14, 1083-1100 (2005)

[5] H. Duflo, B. Morvan, J.-L. Izbicki, "Interaction of Lamb waves on bonded composite plates with defects", Composite Structures 79, 229-233 (2007)

[6] B. Morvan, J.-L. Izbicki, "Defects detection on a composite structure by an optical measurement of ultrasonic surface waves", Pacs reference 43.35.Zc

[7] A.H. Nayfeh, D.E Chimenti, "Free wave propagation in plates of general anisotropic media", Journal of applied Mechanics, vol. 56, 881-886 (1989)

[8] J. L. Rose, "Ultrasonic waves in Solid Media" (Cambridge: Cambridge University Press), (1999)